J|A|C|S
ARTICLES
Published on Web 08/26/2006

Determining the Intracellular Transport Mechanism of a Cleft−[2]Rotaxane

Xiaofeng Bao,[†] Idit Isaacsohn,[‡] Angela F. Drew,[‡] and David B. Smithrud*,[†]

Contribution from the Department of Chemistry, University of Cincinnati, Cincinnati, Ohio 45221, and the Department of Genome Science, University of Cincinnati, Cincinnati, Ohio 45237

Received May 25, 2006; E-mail: david.smithrud@uc.edu

Abstract: Rotaxanes are a class of interlocked compounds that have been extensively investigated for their potential utility as switches or sensors. We recently demonstrated that rotaxanes have further application as agents that transport material into cells. This novel finding prompted our investigation into the mechanism by which rotaxanes are involved in transmembrane transport. Two-dimensional NMR analysis showed that a cleft-containing rotaxane exists in two dominant conformations ("closed" and "open"). To determine the importance of conformational flexibility on the ability of the rotaxanes to bind guests and transport material into cells, the rotaxane was chemically modified to lock it in the closed conformation. Charged guests interact less favorably with the locked rotaxane, as compared to the unmodified rotaxane, both in an aqueous solution and in DMSO. In a chloroform solution, both rotaxanes bind the guests with similar affinities. The locked rotaxane exhibited a reduced capacity to transport a fluoresceinated peptide into cells, whereas the unmodified rotaxane efficiently delivers the peptide. Flow cytometry experiments demonstrated that a high percentage of the cells contained the delivered peptide (89−98%), the level of delivery is concentration dependent, and the rotaxanes and peptide have low toxicity. Cellular uptake of the peptide was largely temperature and ATP independent, suggesting that the rotaxane−peptide complex passes through the cellular membrane without requiring active cell-mediated processes. The results show that the sliding motion of the wheel is necessary for the delivery of materials into cells and can enhance the association of guests. These studies demonstrate the potential for rotaxanes as a new class of mechanical devices that deliver a variety of therapeutic agents into targeted cell populations.

Introduction

Proteins perform many complex processes that are necessary for cell survival.[1] The industrial and medical uses of proteins, however, are limited by their chemical and biological instability, low bioavailability, and high manufacturing costs.[2−6] To overcome these limitations, extensive research has focused on discovering the key features of protein structures that enable them to perform their functions and the means by which these features can be incorporated into synthetic scaffolds.[7−11] Rotaxanes comprise a class of interlocked molecules containing a wheel threaded onto an axle with blocking groups on the ends to keep the wheel from sliding off (Figure 1). The unique ability of the wheel to slide along the axle makes rotaxanes a highly suitable choice for developing molecular switches and sensors.[12] We have previously generated rotaxanes with a synthetic host as one of the blocking groups to create protein mimetics.[13−15] The unique interactions between the wheel and a selected host-blocking group determine the properties of the host−rotaxane complex.

We have previously shown that host−[2]rotaxanes (HRs), containing an arginine-derivatized dibenzyl-24-crown-8 (DB24C8)

[†] Department of Chemistry.
[‡] Department of Genome Science.

(1) Kinbara, K.; Aida, T. *Chem. Rev.* **2005**, *105*, 1377−1400.
(2) Bilati, U.; Allemann, E.; Doelker, E. *Eur. J. Pharm. Biopharm.* **2005**, *59*, 375−388.
(3) Wang, W. *Int. J. Pharm.* **2005**, *289*, 1−30.
(4) Cunha, T.; Aires-Barros, R. *Mol. Biotechnol.* **2002**, *20*, 29−40.
(5) Choi, W. S.; Murthy, G. G. K.; Edwards, D. A.; Langer, R.; Klibanov, A. M. *Proc. Natl. Acad. Sci. U.S.A.* **2001**, *98*, 11103−11107.
(6) Wei, W. *Int. J. Pharm.* **1999**, *185*, 129−188.
(7) Moriuchi, T.; Hirao, T. *Chem. Soc. Rev.* **2004**, *33*, 294−301.
(8) Loughlin, W. A.; Tyndall, J. D. A.; Glenn, M. P.; Fairlie, D. P. *Chem. Rev.* **2004**, *104*, 6085−6117.
(9) Hamuro, Y.; Calama, M. C.; Park, H. S.; Hamilton, A. D. *Angew. Chem., Int. Ed. Engl.* **1997**, *36*, 2680−2683.
(10) Hauert, J.; Fernandez-Carneado, J.; Michielin, O.; Mathieu, S.; Grell, D.; Schapira, M.; Spertini, O.; Mutter, M.; Tuchscherer, G.; Kovacsovics, T. *ChemBioChem* **2004**, *5*, 856−864.
(11) Causton, A. S.; Sherman, J. C. *J. Pept. Sci.* **2002**, *8*, 275−282.
(12) For recent examples, see: (a) Braunschweig, A. B.; Northrop, B. H.; Stoddart, J. F. *J. Mater. Chem.* **2006**, *16*, 32−44. (b) Tian, H.; Wang, Q. C. *Chem. Soc. Rev.* **2006**, *35*, 361−374. (c) Moonen, N. N. P.; Flood, A. H.; Fernandez, J. M.; Stoddart, J. F. *Top. Curr. Chem.* **2005**, *262*, 99−132. (d) Kay, E. R.; Leigh, D. A. *Top. Curr. Chem.* **2005**, *262*, 133−177. (e) Berna, J.; Leigh, D. A.; Lubomska, M.; Mendoza, S. M.; Perez, E. M.; Rudolf, P.; Teobaldi, G.; Zerbetto, F. *Nat. Mater.* **2005**, *4*, 704−710. (f) Ghosh, P.; Federwisch, G.; Kogej, M.; Schalley, C. A.; Haase, D.; Saak, W.; Lutzen, A.; Gschwind, R. M. *Org. Biomol. Chem.* **2005**, *3*, 2691−2700. (g) Credi, A.; Ferrer, B. *Pure Appl. Chem.* **2005**, *77*, 1051−1057. (h) Collin, J. P.; Jouvenot, D.; Koizumi, M.; Sauvage, J. P. *Eur. J. Inorg. Chem.* **2005**, 1850−1855. (i) Qu, D. H.; Wang, Q. C.; Tian, H. *Angew. Chem., Int. Ed.* **2005**, *44*, 5296−5299. (j) Leigh, D. A.; Morales, M. A. F.; Perez, E. M.; Wong, J. K. Y.; Saiz, C. G.; Slawin, A. M. Z.; Carmichael, A. J.; Haddleton, D. M.; Brouwer, A. M.; Buma, W. J.; Wurpel, G. W. H.; Leon, S.; Zerbetto, F. *Angew. Chem., Int. Ed.* **2005**, *44*, 3062−3067.
(13) Dvornikovs, V.; House, B. E.; Kaetzel, M.; Dedman, J. R.; Smithrud, D. B. *J. Am. Chem. Soc.* **2003**, *125*, 8290−8301.
(14) Smukste, I.; House, B. E.; Smithrud, D. B. *J. Org. Chem.* **2003**, *68*, 2559−2571.
(15) Smukste, I.; Smithrud, D. B. *J. Org. Chem.* **2003**, *68*, 2547−2558.

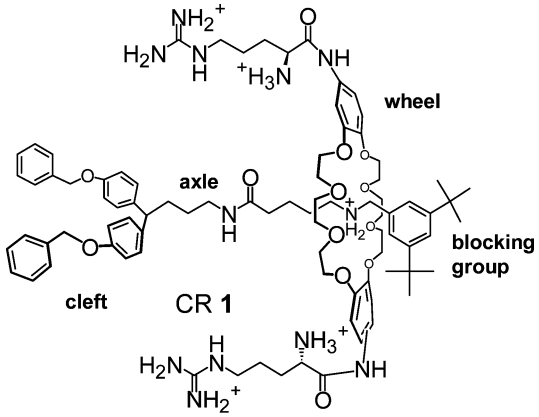

Figure 1. The binding domain of cleft-[2]rotaxane **1** comprises the aromatic surfaces of the cleft and both the aromatic surfaces and the arginine moieties of the wheel.

ring as the wheel and a calix[4]arene, cyclophane, or cleft (cleft−[2]rotaxane (CR) **1**) as a blocking group, bind a variety of guests in DMSO, water, and mixed solvent systems with large association constants.[13,14] The binding domain of the rotaxanes is divided between one blocking group (calix[4]arene, cyclophane, or cleft) and the wheel. For example, the binding domain of CR **1** (Figure 1) comprises the aromatic surfaces of the cleft and both the aromatic surfaces and the arginine moieties of the wheel. We have shown that the aromatic ring and the arginine moiety of the DB24C8 wheel can interact favorably with a guest.[13,14] One unique feature of the rotaxane architecture for pocket formation is that when a guest binds, the wheel adjusts its position on the axle to form the most stable conformation.[15] The advantage of host−rotaxanes, as compared to other hosts which bind small peptides,[16] is that they can deliver materials into cells. For example, CR **1** delivers fluorescein into COS-7 cells.[13] The purpose of the current study is to determine the mechanism used by the transporters to deliver biologically relevant peptides through the cell membrane and the features of the rotaxanes that enable this process to occur. Determining the transport mechanism is an important step in the development of HRs that efficiently and selectively transport material into targeted cells. These mechanical transporters would be a valuable addition to the emerging set of mechanical devices that are based on rotaxanes.[12]

In our original study of CR **1**, we observed a minimal solvent dependency on the degree of association for guests of various polarities.[13] One-dimensional NMR analysis of a phenylalanine−rotaxane in DMSO-d_6 showed that the dominant conformation has the wheel closer to the pocket because of a strong noncovalent bond between the carboxylate of phenylalanine and an arginine moiety of the wheel.[15] Based on these results, we postulated that the wheel slides along the axle with a change in the environment to maintain the most stable host−guest complex. This ability of a rotaxane to adopt multiple stable complexes is likely responsible for the observed intracellular transport because the delivery of materials into cells requires the complex to remain stable in environments of a wide range of polarities.[17] To test this hypothesis, a comparison was made of the preferred conformations, the binding abilities, and the transport abilities of CR **1** versus the same rotaxane after chemical modification to prevent the wheel from sliding.

Results and Discussions

Rotaxane Conformation Determination via Multidimensional NMR Analysis. NOESY (or ROESY) experiments are an ideal method to determine the position of the wheel on the axle because the Nuclear Overhauser Effect (NOE) signals show which protons are close together in space. COSY and TOCSY experiments are used to aid in the proton assignments. These NMR experiments were performed on solutions containing CR **1** with and without fluorescein. CR **1** was chosen because it has a simpler ^{1}H NMR spectrum than the other rotaxanes available in our group, making its proton assignment more reliable. Fluorescein was chosen as the representative guest because it strongly associates with CR **1**, its ^{1}H NMR signals do not overlap with CR **1**, and, once linked to a guest peptide, its emission spectra enable detection in cellular transport assays. Water and chloroform solutions were chosen to represent the polar extracellular environment and the lipid portion of cell membranes, respectively. DMSO was added to enhance the solubility of CR **1**.

The driving force for the formation of rotaxanes, such as CR **1**, is the attraction between the ammonium ion of the axle and the electron-rich oxygen atoms of the wheel.[18,19] Thus, we predicted in 95% $CDCl_3$/5% DMSO-d_6 the predominant conformation of the rotaxanes would have the wheel existing over the axle's ammonium ion. This arrangement, the open conformation, was observed in the analysis of the NOESY spectra. NOE cross-peaks were observed between the blocking group and the crown ether's CH_2 protons (Figure 2 and Supporting Information). The open conformation is maintained in the presence of fluorescein; however, different protons are coupled than those in the unbound state, i.e., without fluorescein. Cross-peaks existed between the aromatic protons of the blocking group and the wheel and between the crown ether's CH_2 protons and the benzylic protons of the axle. Without fluorescein, only the aliphatic moieties of the crown ether ring are close to the blocking group. With fluorescein, at least one aromatic ring of the crown is positioned close to the blocking group. This suggests that the S-shaped conformation[20] of the crown exists in the bound state and one aromatic ring covers the blocking group. The other ring is pointed toward fluorescein presumably due to bond formation between the ring's arginine moiety and the carboxylate of fluorescein. NOE cross-peaks were also observed between fluorescein and the aromatic cleft, which shows that fluorescein resides within the cleft. This suggests that aromatic moieties remain in the pocket during the passage through the cellular membrane. Modification of the cleft may lead to more efficient delivery devices through more stable complex formation in water and in the lipid bilayer.

(16) Hortala, M. A.; Fabbrizzi, L.; Marcotte, N.; Stomeo, F.; Taglietti, A. *J. Am. Chem. Soc.* **2003**, *125*, 20−21. (b) Tsubaki, K.; Kusumoto, T.; Hayashi, N.; Nuruzzaman, M.; Fuji, K. *Org. Lett.* **2002**, *4*, 2313−2316. (c) Rensing, S.; Schrader, T. *Org. Lett.* **2002**, *4*, 2161−2164. (d) Ait-Haddou, H.; Wiskur, S. L.; Lynch, V. M.; Anslyn, E. V. *J. Am. Chem. Soc.* **2001**, *123*, 11296−11297. (e) Mizutani, T.; Wada, K.; Kitagawa, S. *J. Am. Chem. Soc.* **1999**, *121*, 11425−11431.

(17) Avdeef, A. *Absorption and Drug Development: solubility, permeability, and charge state*; Wiley-Interscience: Hoboken, NJ, 2003; Chapter 5.

(18) Ramero, C.; Guadarrama, P.; Fomine, S. *J. Mol. Model.* **2005**, *12*, 85−92.

(19) Zehnder, D; Smithrud, D. B. *Org. Lett.* **2001**, *16*, 2485−2486.

(20) (a) Loeb, S. J.; Tiburcio, J.; Vella, S. J. *Org. Lett.* **2005**, *7*, 4923−4926. (b) Hubbard, A. L.; Davidson, G. J. E.; Patel, R. H.; Wisner, J. A.; Loeb, S. J. *Chem. Commun.* **2004**, 138−139. (c) Ashton, P. R.; Campbell, P. J.; Chrystal, E. J. T.; Glink, P. T.; Menzer, S.; Philp, D.; Spencer, N.; Stoddart, J. F.; Tasker, P. A.; Williams, D. J. *Angew. Chem., Int. Ed. Engl.* **1995**, *34*, 1865−1869.

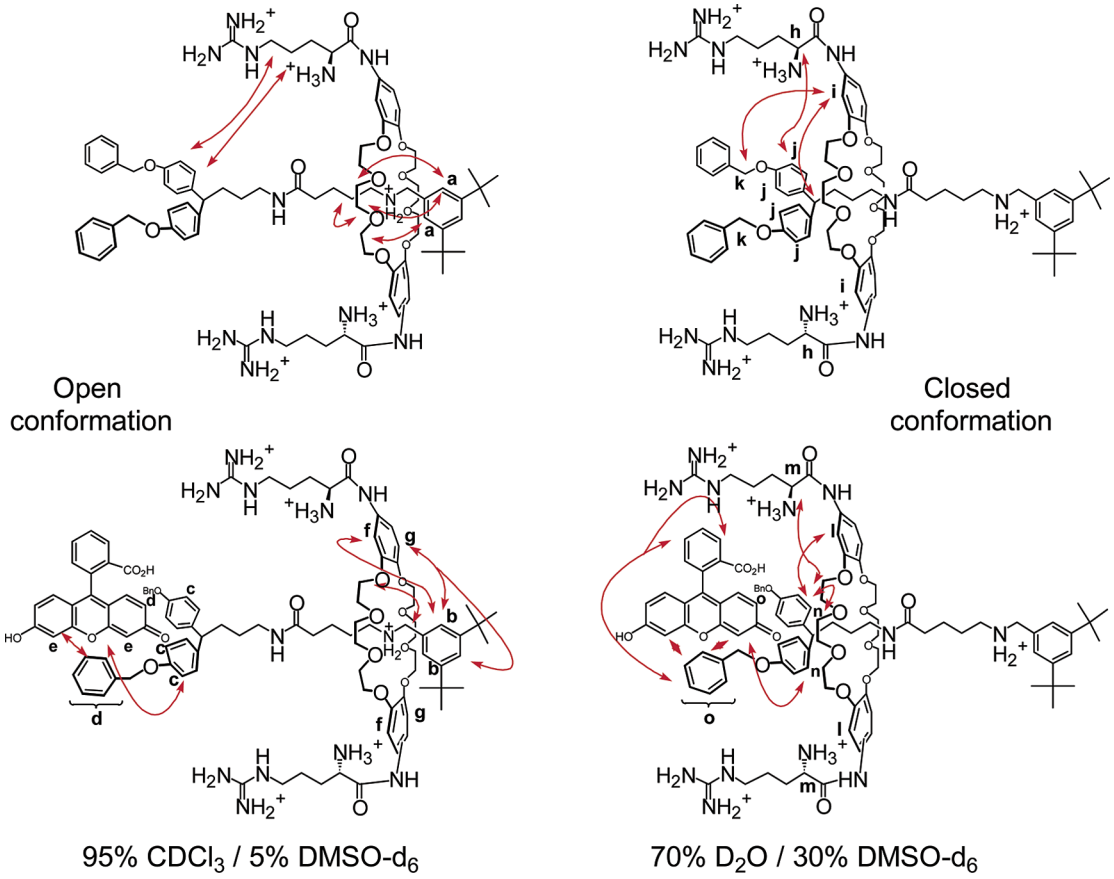

Figure 2. Analysis of NOESY spectra shows that the open and closed conformations of CR **1** are dominant in an apolar and aqueous environment, respectively. The double-headed arrows show the coupled protons between the wheel and the axle of CR **1**. Lower case letters indicate chemically equivalent protons.

A different rotaxane conformation would be expected to dominate in an aqueous environment since the attraction of the ammonium ion of the axle for the wheel's oxygen atoms is weakened by hydrogen bond (H-bond) formation with water molecules.[20c,21] Also, the aromatic and aliphatic surfaces of the wheel and the pocket will associate in accordance with the hydrophobic effect.[22] Both factors favor the existence of a "closed" conformation, which refers to the state whereby the wheel exists close to the pocket (Figure 2). The NOESY (and ROESY) spectrum of CR **1** in a polar solvent (70% D_2O/30% DMSO-d_6) shows NOE cross-peaks between the wheel and the pocket (Supporting Information), which is consistent with the closed conformation being dominant.

The hydrophobic binding domain that is produced in the closed conformation should be optimal for the sequestering of aromatic or aliphatic moieties of a guest. NOE cross-peaks are observed between fluorescein and the aromatic pocket, which shows that fluorescein is bound within the pocket (Figure 2 and Supporting Information). The closed conformation is dominant when fluorescein is bound to the rotaxane. Although NOE signals are observed between several protons of the wheel and the pocket in the bound state, the coupled protons are different than the ones observed in the unbound state. Not surprisingly, the wheel adjusts its conformation to admit fluorescein into the pocket. The loss of the NOE signal between the wheel's aromatic ring and the benzylic protons of the pocket is consistent with the wheel residing further away from the pocket in the bound state.

The arginine moieties of the CRs most likely perform multiple roles in the transport process. It is attracted to the phosphate groups on the cell surface, covers the negatively charged groups of a guest during the passage through the lipid layer, and may or may not form a salt-bridge with a guest in the aqueous phase outside a cell. In nonaqueous environments, such as the cell surface and the lipid layer, multiple noncovalent interactions (e.g., salt bridge[23a] and cation-π interaction[23a,b] with the arginine moieties and aromatic stacking interactions[24]) most likely contribute to complex formation in apolar environments. In aqueous phases, however, guests with charged or polar functional groups will experience weak charge−charge or H-bond interactions with the rotaxane's arginine moieties because of the strong solvation energy of water.

In the open conformation, the γ- and δ-protons of an arginine moiety are coupled to protons on a cleft's aromatic ring (Figure 2). Thus, at least one arginine moiety is extended toward the pocket. These NOEs disappear when CR **1** is bound to fluorescein. Most likely, formation of a salt-bridge between the carboxylate of fluorescein and the guandinium moiety of the wheel repositions the arginine moiety in space. In the closed conformation, NOEs are observed between the aromatic and

(21) Cantrill, S. J.; Pease, A. R.; Stoddart, J. F. *J. Chem. Soc., Dalton Trans.* **2000**, *21*, 3715−3734.
(22) Xu, H. F.; Dill, K. A. *J. Phys. Chem. B* **2005**, *109*, 23611−23617. (b) Dill, K. *Biochemistry* **1990**, *29*, 7133−7155.
(23) (a) Gallivan, J. P.; Dougherty, D. A. *J. Am. Chem. Soc.* **2000**, *122*, 870−874. (b) Ma, J. C.; Dougherty, D. A. *Chem. Rev.* **1997**, *97*, 1303−1324.
(24) Pang, Y. P.; Miller, J. L.; Kollman, P. A. *J. Am. Chem. Soc.* **1999**, *121*, 1717−1725.

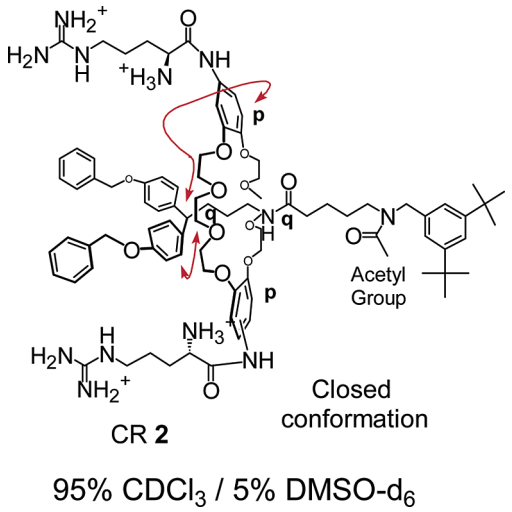

Figure 3. CR **1** was acetylated to create rotaxane CR **2** that is effectively locked in the closed conformation. The double-headed arrows show the coupled protons between the wheel and the axle of CR **2**, indicating that CR **2** is in the closed conformation. Lower case letters indicate chemically equivalent protons.

arginine moieties of the wheel and the aromatic and benzylic protons of the cleft. The α-proton of arginine is coupled to an aromatic cleft proton, whereas, in the open conformation, the γ- and δ-protons of an arginine moiety are coupled to protons on a cleft's aromatic ring. This confirms that in the closed conformation at least one arginine moiety is positioned closer to the pocket than in the open conformation. The α-H of arginine and the aromatic cleft, however, remain close when fluorescein is bound. This suggests that the position of this arginine is not significantly changed when fluorescein is bound. Either the arginine moiety is preorganized to bind fluorescein or it does not interact with fluorescein. These results show that an arginine moiety can interact with a guest in the open and closed conformation. We discuss later that the close association of the arginine with the cleft that exists in the closed conformation most likely is responsible for weak complex formation in DMSO and disrupts the transport process.

Creation of a Locked Rotaxane. CR **1** was chemically modified to create a rotaxane that is effectively locked in the closed conformation (CR **2**, Figure 3). Acetylation of the nitrogen atom of the axle (Supporting Information) reduces its ability to interact favorably with the wheel's oxygen atoms; combined with the added steric hindrance, the wheel is forced closer to the cleft. NOE cross peaks existed between the aromatic protons of the wheel and the CH proton of the cleft and between the CH_2 protons of the wheel and the aromatic protons of the cleft. Thus, 2D NMR analysis verified that CR **2** exists in a closed conformation in an apolar solution 95% $CDCl_3$/5% DMSO-d_6 (Supporting Information). CR **1**, on the other hand, exists predominantly in an open conformation in this solution.

Determination of the Binding Capacity of the Rotaxanes. According to the two conformation model, CR **2** being in the locked conformation should bind guests as well as or better than CR **1** in aqueous environments and worse in apolar environments. To explore the binding properties of the rotaxanes, a series of guests were chosen that have different physical properties. Fluorescein contains a large aromatic surface and several negatively charged functional groups in buffered water (pH 7.0). *N*-Acetylated tryptophan (Ac-Trp) is also negatively charged in buffered water (pH 7.0), but it has a smaller aromatic surface. Pyrene was chosen to test the abilities of the rotaxanes to bind a large aromatic surface. Fl-Ala-Val-Trp-Ala-Leu-$CONH_2$ (Fl-AVWAL) contains fluorescein and tryptophan moieties and will be used in the transport assays. These guests were also chosen because they are fluorescent. Because a guest's fluorescence is quenched when it is complexed by a host−rotaxane, fluorescence quenching assays were performed to obtain the association constants (K_A's) of the CR−guest complexes. The assay involves adding small aliquots of a rotaxane to a solution of a guest at a known concentration and monitoring the degree of quenching. Association constants were derived by performing nonlinear least-squares analysis of plots that compare the degree of quenching versus the concentration of a rotaxane, as previously described.[25]

Table 1. Association Constants for CR-Guest Complexes ($K_A \times 10^{-3}$)[a]

guest	solvent	$K_{A,CR1}$[b]	$K_{A,CR2}$[c]	$K_{A,CR1}/K_{A,CR2}$
Ac-Trp	water[d]	24	9	2.8
	DMSO	22	16	1.4
	$CHCl_3$[e]	45	53	0.85
fluorescein	water	53	14	3.8
	DMSO	770	5	150
	$CHCl_3$	56	64	0.88
Fl-AVWAL[f]	water	360	50	7.2
	DMSO	600	18	33
	$CHCl_3$	50	50	1.0
pyrene	water	40	120	0.33
	DMSO	17	4	4.2
	$CHCl_3$	17	21	0.81

[a] The assays were performed at room temperature; the standard deviation is less than 10% for each K_A. [b] K_A for CR **1** complexes. [c] K_A for CR **2** complexes. [d] 98% water (PBS 1 mM, pH 7.0)/2% DMSO. [e] 98% $CHCl_3$/2% DMSO. [f] Fl-Ala-Val-Trp-Ala-Leu-$CONH_2$.

A dramatic difference in affinity is observed for the complexes of fluorescein and the CRs in DMSO (Table 1). According to molecular modeling results, fluorescein can interact simultaneously with the pocket and a guanidinium moiety in either the closed or open conformation (Supporting Information). The major difference is observed for the conformations without fluorescein. In the open conformation, the guanidinium moiety is positioned too far away to interact strongly with the pocket. The CH_2's of the arginine's side chain are still close enough to the pocket to produce the observed NOE signals (Figure 2). In the closed conformation, on the other hand, the guanidinium moiety is positioned within the pocket. The weaker association observed for CR **2** and fluorescein is most likely a result of the guanidinium moiety and fluorescein competing for the pocket. Binding of fluorescein breaks the favorable guanidinium-pocket bond (cation−π interaction[23]), which reduces the overall favorable binding energy. We have observed that strong interactions can occur between functional groups on the blocking group and the wheel.[15] A similar difference in complex stability is not observed for the other guests in DMSO. Perhaps the guanidinium group remains in the pocket in the complexes of Ac-Trp and pyrene: the small indole ring of Ac-Trp resides within the benzyl groups of the pocket, and pyrene shares the guanidinium moiety with the pocket. Whatever the reason for the observed differences in the K_A's, these results show that

(25) Conners, K. A. *Binding Constants, The Measurement of Molecular Complex Stability*; Wiley: New York, 1987.

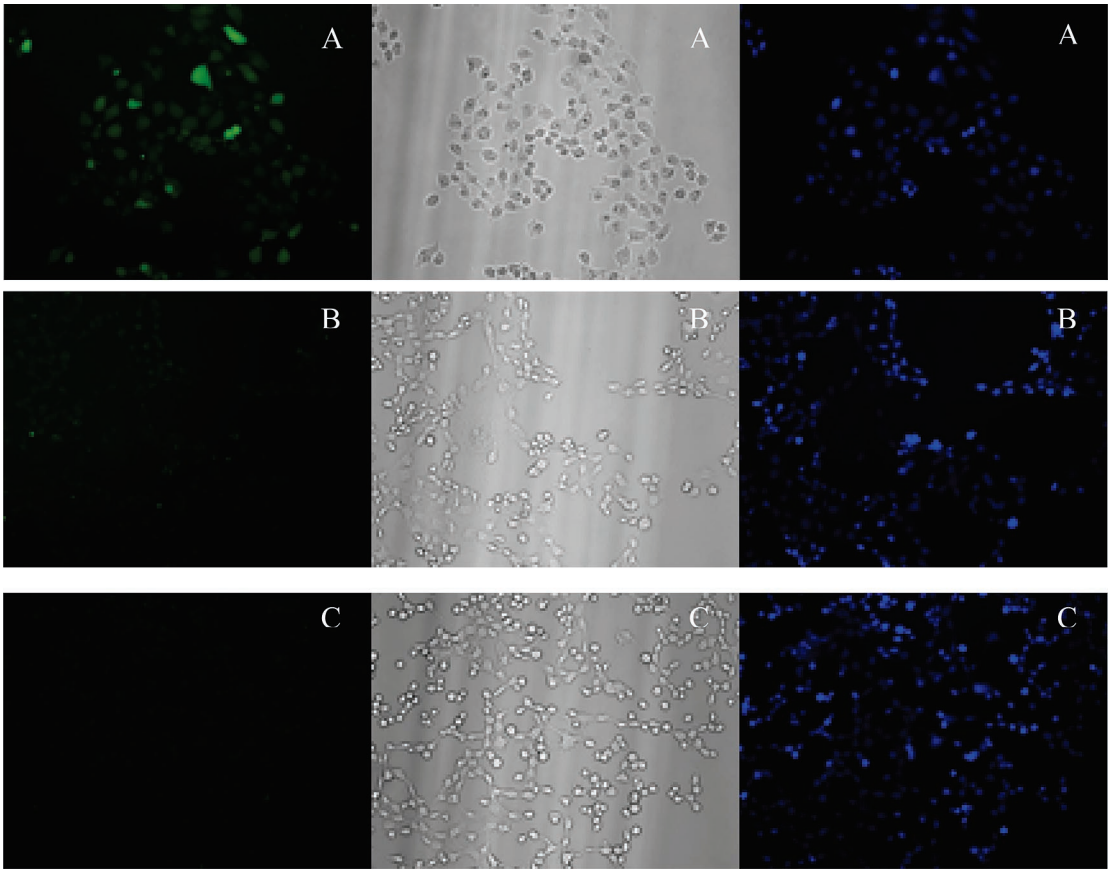

Figure 4. Fluorescence microscopy of COS-7 cells incubated with rotaxanes. Cells were viewed for FITC fluorescence (Fl-AVWAL uptake; left panels), white light (middle panels), and calcein blue fluorescence (viability; right panels). Uptake of fluorescent peptide is greatest with CR **1** and Fl-AVWAL (A) and markedly less with CR **2** and Fl-AVWAL (B) or with Fl-AVWAL alone (C). Cell viability is similar for each combination of rotaxane and Fl-AVWAL: ([CR **1**] = 10 μM or [CR **2**] = 20 μM), Fl-AVWAL (10 μM), and calcein blue (original magnification: 100×).

the cleft−rotaxane can be a guest-selective binding agent as a result of subtle differences in the orientation of its functional groups.

A large difference in complex strength is also observed for the binding of Fl-AVWAL by CR **1** as compared to CR **2** in DMSO. The fluorescein, tryptophan, or one of the aliphatic moieties of Fl-AVWAL could be bound within the cleft. CR **1** binds Fl-AVWAL and fluorescein with similarly large K_A values (6.0×10^5 M^{-1} and 7.7×10^5 M^{-1}, respectively), which suggests that CR **1** binds the fluorescein moiety of Fl-AVWAL. In the case of CR **2**, similar K_A's are observed for the complexes of CR **2**·Fl-AVWAL and CR **2**·Ac-Trp ($K_A = 1.8 \times 10^4$ and 1.6×10^4 M^{-1}, respectively). CR **2** weakly associates with fluorescein ($K_A = 5 \times 10^3$ M^{-1}). Therefore, the tryptophan moiety of Fl-AVWAL is most likely bound to CR **2** and not the fluorescein ring. An exposed, negatively charged fluorescein moiety in the CR **2**·Fl-AVWAL complex could hamper the transport of Fl-AVWAL into cells.

According to NMR analysis, the closed conformation dominates in an aqueous environment. This conformation should be optimal for the binding of hydrophobic guests. Thus, CR **2** should have larger K_A's in aqueous environments since a greater percentage of rotaxanes are in the closed conformation as compared to CR **1**, whose wheel is constantly sliding back and forth over the axle. Pyrene is bound by CR **2** in 98% water/2% DMSO more favorably than by CR **1** (Table 1). This result demonstrates that the closed conformation is optimal for the binding of hydrophobic guests. On the other hand, CR **2** forms slightly weaker complexes with Ac-Trp and fluorescein than does CR **1**. Possibly weak, favorable interactions occur between these guests and the arginine moieties of CR **1**, but not for CR **2** in an aqueous environment. The open conformation, available only to CR **1**, could be involved in complex formation with a guest in aqueous environments if the sliding rate is faster than the off rate of the guest. If true, this demonstrates that there is a dynamic component to the association event. The free energy for the association of Fl-AVWAL by CR **1** is more exergonic than the value observed for fluorescein or Ac-Trp. The additional free energy could arise from Fl-AVWAL forming a bent structure that enables both aromatic surfaces to interact simultaneously with CR **1**. Another possibility is that less energy is required to remove water molecules from Fl-AVWAL than fluorescein. The high solubility in water of these guests prevents us from investigating the latter possibility.

Similar affinities are observed for the binding of CR **1** and CR **2** to fluorescein, Fl-AVWAL, and Ac-Trp in 95% $CHCl_3$/5% DMSO. Their K_A's are twice as large as that obtained for the binding of pyrene. Most likely, the dominant interaction is a strong salt-bridge between the arginine moieties of the wheel and the carboxylate of these guests. Another possibility is that proton transfer occurs between the carboxylate of a guest and a guanidinium of the rotaxane. In this case a strong H-bond would drive complex formation. Evidence for the formation of neutral complexes is seen in the ab initio and semiempirical calculations of complexes between methylguanidinium and acetates, which showed that neutral complexes are more stable

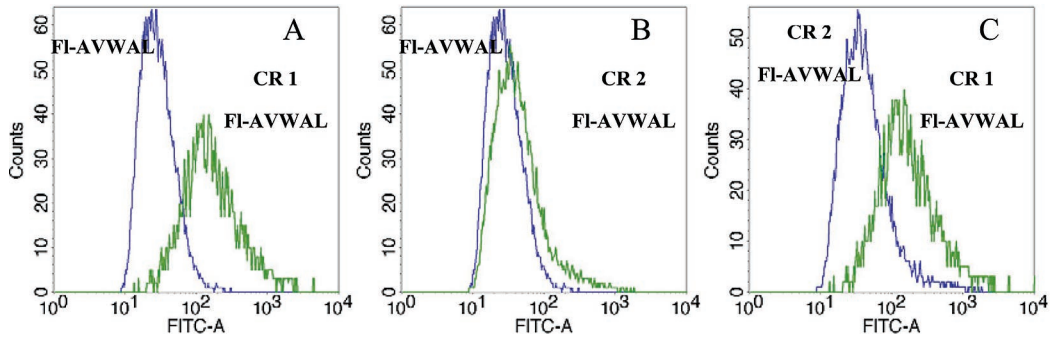

Figure 5. Relative fluorescence (FITC) of COS-7 cells exposed to (A) Fl-AVWAL alone vs CR **1** and Fl-AVWAL, (B) Fl-AVWAL alone vs CR **2** and Fl-AVWAL, and (C) CR **1** and Fl-AVWAL vs CR **2** and Fl-AVWAL by flow cytometry. Cells were incubated with [Fl-AVWAL] = 10 μM, [CR **1**] = 10 μM, or [CR **2**] = 20 μM in PBS (pH 7.4) for 1 h at 20 °C.

than the zwitterionic pair in a solvent-free environment.[26] Thus, the neutral complex most likely exists when the CR **1**−Fl-AVWAL complex passes through the aliphatic chains of the cell membrane.

Cellular Transport Efficiencies of the Rotaxanes. Since the dominant conformation of the host−[2]rotaxanes depends on the environment, these conformational states should contribute to the transportation of guests into cells, i.e., transport from a polar environment through the apolar cell membrane.[17] To test this hypothesis, we determined the abilities of CR **1** and CR **2** to transport Fl-AVWAL into COS-7 cells, via fluorescence detection. Fl-AVWAL was selected since it contains functional groups of all polarities, which provides a stringent test of the transport abilities of the CR's. The cells were incubated with CR **1** or CR **2** in PBS for 30 min before Fl-AVWAL was added since pilot studies showed that preincubation with CR **1** increased the uptake of Fl-AVWAL (data not shown). After an additional hour, the cells were washed thoroughly, and calcein blue AM was added to each well to demonstrate cell viability or potential toxicity after incubation with rotaxanes and peptides. Calcein blue is a cell permeable ester that is hydrolyzed to its acidic form in live cells via enzymatic proteolysis and emits a blue fluorescence signal.[27] Trypsin digestion was used to lift the cells from the wells and to remove any residual Fl-AVWAL nonspecifically attached to the outer cellular membrane.[28a] Cellular delivery of Fl-AVWAL and viability were visualized using fluorescence microscopy, and the relative fluorescence intensity of these cells was quantified by multicolor flow cytometry (BD FacsAria).

For the cellular assays, up to 20 μM CR **1**, CR **2**, and Fl-AVWAL were chosen to ensure complexation occurs in the aqueous phase and to minimize toxicity. High and moderate fluorescence was observed in cells that were exposed to Fl-AVWAL (10 μM) and CR **1** (10 μM) (Figures 4a). Cells exposed to CR **2** (10 μM) and Fl-AVWAL (10 μM), on the other hand, were only weakly fluorescent, similar to that of Fl-AVWAL alone (Figure 4c). A low level of emission was observed when the concentration of CR **2** was increased to 20 μM (Figure 4b). Strong calcein blue fluorescence was observed in the majority of cells regardless of treatment.

Flow cytometry was used to quantify the relative levels of Fl-AVWAL and calcein blue within the cells. Thresholds and gates were set as described in the experimental section and applied to each sample. CR **1** efficiently delivered Fl-AVWAL

Table 2. Quantification of Fl-AVWAL Uptake in COS-7 Cells by Flow Cytometry

compound(s)[a]	%high FITC cells	%low FITC cells	total %FITC cells	%cbAM[b] cells
CR **1** + Fl-AVWAL	31	59	90	90
CR **2** + Fl-AVWAL	1.6	21	23	80
CR **1**	0.3	4.1	4.4	81
CR **2**	0	1.3	1.3	90
Fl-AVWAL	0.3	4.9	5.2	86
none	0	1.0	1.0	94

[a] [CR **1**] = 10 μM, [CR **2**] = 20 μM, [Fl-AVWAL] = 10 μM; all transport assays were performed in PBS (pH 7.4) for 1 h. [b] [calcein blue AM] = 1 μM.

Table 3. Flow Cytometric Analysis of Intracellular Delivery of CR **1**·Fl-AVWAL after Concentration, ATP, and Temperature Reduction

treatment[a]	CR **1** (M)	Fl-AVWAL (M)	%high FITC cells	%low FITC cells	total %FITC cells	%cbAM cells
20 °C	10	20	40	58	98	90
	10	10	31	59	90	81
	5	20	20	79	89	90
	5	10	4	85	89	88
	0	20	0.3	4.9	5	86
	0	0	0	1	1	94
ATP depletion	10	20	6	67	73	89
	10	10	6	52	58	42
	5	10	1	51	52	83
	0	10	0.5	3.9	4	71
	0	0	0	5.0	5	76
4 °C	10	20	13	68	81	90
	10	10	13	63	76	90
	5	10	2	55	57	91
	0	10	0.3	5.4	6	74
	0	0	0	4.4	4	78

[a] Assay was performed in PBS (pH 7.4) for 1 h.

(26) Melo, A.; Ramos, M. J.; Floriano, W. B.; Gomes, J. A. N. F.; Leao, J. F. R.; Magalhaes, A. L.; Maigret, B.; Nascimento, M. C.; Reuter, N. *THEOCHEM* **1999**, *463*, 81−90.

(27) (a) Morley, N.; Rapp, A.; Dittmar, H.; Salter, L.; Gould, D.; Greulich, K. O.; Curnow, A. *Mutagenesis* **2006**, *21*, 105−114. (b) Komarova, S. V.; Pilkington, M. F.; Weidema, A. F.; Dixon, S. J.; Sims, S. M. *J. Biol. Chem.* **2003**, *278*, 8286−8293. (c) Dimitrov, A. S.; Xiao, X.; Dimitrov, D. S.; Blumenthal, R. *J. Biol. Chem.* **2001**, *276*, 30335−30341. (d) Krasnow, M. A.; Cumberledge, S.; Manning, G.; Herzenberg, L. A.; Nolan, G. P. *Science* **1991**, *251*, 81−85.

(28) (a) Richard J. P.; Melikov, K.; Vives, E.; Ramos, C.; Verbeure, B.; Gait, M. J.; Chernomordik, L. V.; Lebleu, B. *J. Biol. Chem.* **2003**, *278*, 585−590. (b) Langel, U. *Cell Penetrating Peptides: Processes and Applications*; CRC Press: Boca Raton, FL, 2002. (c) Suzuki, T.; Futaki, S.; Niwa, M.; Tanaka, S.; Ueda, K.; Sugiura, Y. *J. Biol. Chem.* **2002**, *277*, 2437−2443. (d) Futaki, S.; Suzuki, T.; Ohashi, W.; Yagami, T.; Tanaka, S.; Ueda, K.; Sugiura, Y. *J. Biol. Chem.* **2001**, *276*, 5836−5840. (e) Pooga, M.; Hallbrink, M.; Zorko, M.; Langel, U. *FASEB J.* **1998**, *12*, 67−77. (f) Afonina, E.; Stauber, R.; Pavlakis, G. N. *J. Biol. Chem.* **1998**, *273*, 13015−13021. (g) Vives, E.; Brodin, P.; Lebleu, B. *J. Biol. Chem.* **1997**, *272*, 16010−16017. (h) Derossi, D.; Calvet, S.; Trembleau, A.; Brunissen, A.; Chassaing, G.; Prochiantz, A. *J. Biol. Chem.* **1996**, *271*, 18188−18193.

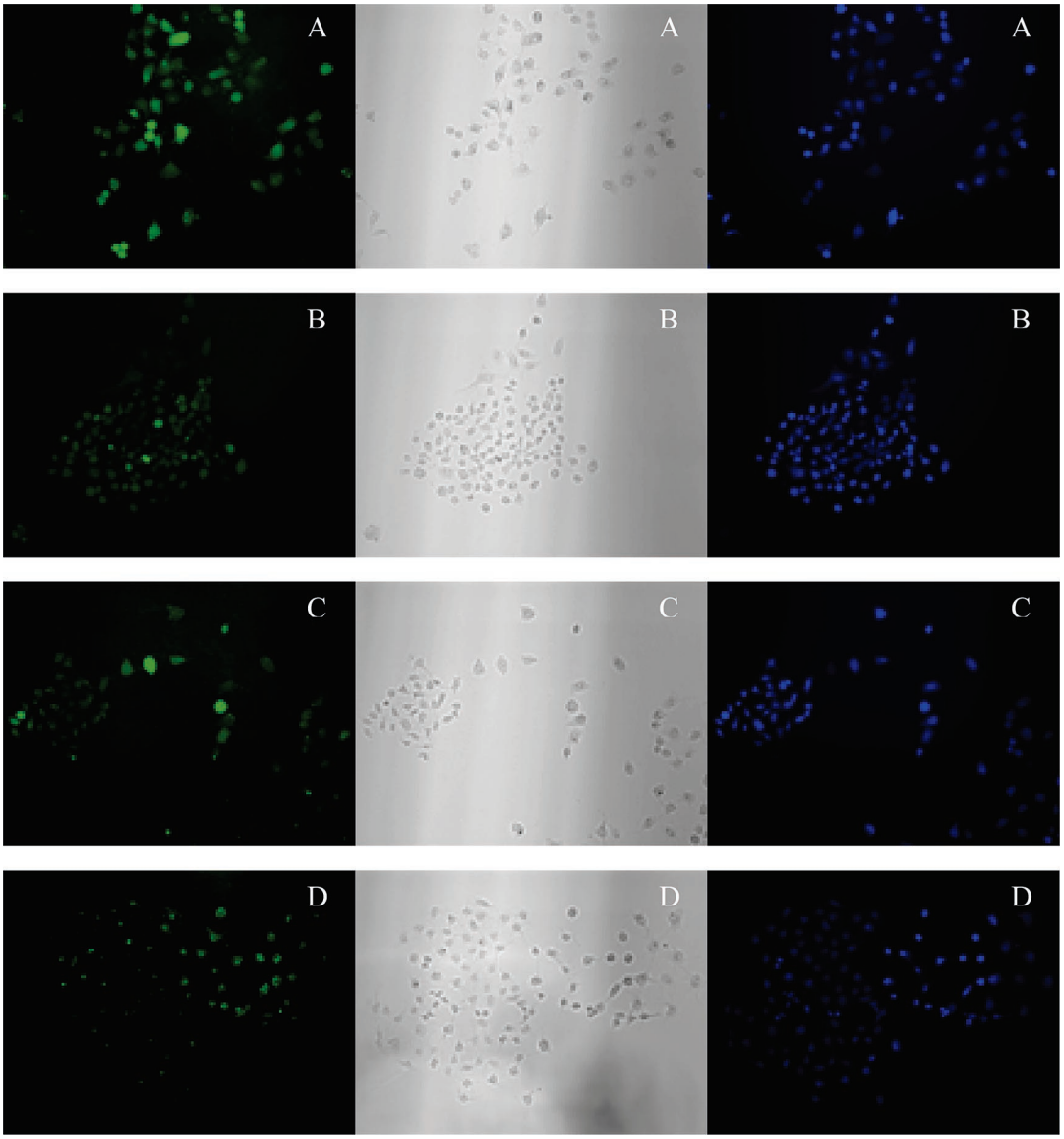

Figure 6. Fluorescence microscopy of COS-7 cells exposed to various concentrations of CR **1** and Fl-AVWAL: (A) 10 μM CR **1** and 20 μM Fl-AVWAL, (B) 10 μM CR **1** and 10 μM Fl-AVWAL, (C) 5 μM CR **1** and 20 μM Fl-AVWAL, and (D) 5 μM CR **1** and 10 μM Fl-AVWAL. Representative pictures are shown: FITC emission of Fl-AVWAL (left panels), white light (middle panels), and calcein blue fluorescence emission (right panels) (original magnification: 100×).

into a large percentage of the cells (90% above background; Figure 5 and Table 2). CR **2** (20 μM) transports Fl-AVWAL into only a small proportion of cells (23%). A high proportion of calcein blue positive cells (range: 80% to 94%) was observed (see also Supporting Information). This demonstrates that both CRs and Fl-AVWAL at these concentrations have a low level of toxicity. Calcein blue and Fl-AVWAL fluorescence were independently expressed in the cells.

Determining the Cellular Transport Mechanism. In order to determine whether endocytosis was the predominant mechanism of intracellular transport, additional experiments were performed at 4 °C or by depleting cellular ATP for 1 h.[28] This method has previously been used to demonstrate that a TAT peptide (derived from the HIV-1 Tat protein) enters cells mainly through the endocytotic pathway.[28a] Cellular ATP was depleted by preincubation with a PBS solution containing 6 mM 2-deoxy-D-glucose and 10 mM sodium azide for 1 h, as previously described.[28a] Since some cell death was caused by this procedure (assessed by cell detachment and loss of calcein blue fluorescence), further analysis was restricted to live cells that remained attached to the plates. On separate plates, temperature reduction was achieved by maintaining cells in PBS at 4 °C for the duration of the assay. Cells were incubated with CR **1** and then Fl-AVWAL for 1 h, observed via inverted fluorescence microscopy (Zeiss Axiovert 200M), then trypsinized, and assessed by flow cytometry. The overall number of FITC positive cells was only slightly reduced by low temperature or ATP depletion (Table 3). For example, the total amount of FITC positive cells was 98%, 81%, and 73% for cells that were untreated, treated at 4 °C, and treated with 2-deoxy-D-glucose and sodium azide, respectively. This indicates that endocytosis is not the major pathway for cell entry. While these studies suggest some cellular involvement in peptide uptake, a highly significant amount of peptide uptake still occurs in cells

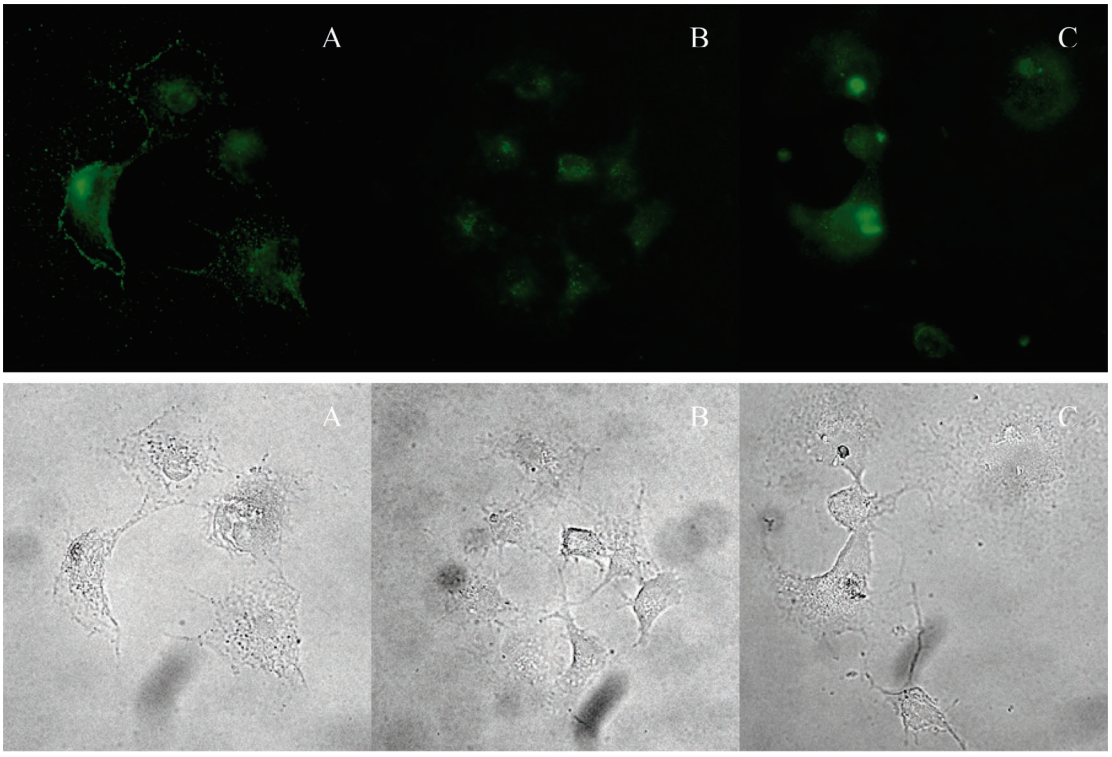

Figure 7. Fluorescence photomicrographs showing three representative examples of COS-7 cells exposed to CR **1** (10 μM) and Fl-AVWAL (10 μM). Fluorescein emission is shown on top, and the same cells under white light are shown on bottom (original magnification: 400×).

immobilized by low temperature or ATP depletion. Clearly the rotaxane alone is largely responsible for most of the intracellular transport of the peptide.

In order to determine the requirement of complex formation for peptide uptake, the effect of varying the concentrations of CR **1** and Fl-AVWAL was assessed (Figure 6). The total percentage of fluorescent cells is not greatly affected by a reduction in the concentration of the components (98% to 89%, Table 3). The proportion of highly fluorescent cells, however, is reduced upon decreasing the concentration of the components. Knowing that Fl-AVWAL does not enter cells unaided, this result is consistent with CR **1** forming a complex with Fl-AVWAL in the extracellular domain and then penetrating the cells. As the concentration of these complexes increase in the extracellular domain, a greater number enter the cells, giving more intensely fluorescent cells. We observed that complex formation quenches the fluorescence emission of Fl-AVWAL in various solvents. If the same quenching phenomenon occurs inside the cells, the existence of fluorescent cells means that a certain percentage of the complexes dissociate within the cells probably because of dilution. There is the possibility that CR **1** could return to the extracellular domain, bind Fl-AVWAL and reenter the cell, and thus possibly reduce the concentration dependence of the observed fluorescence. The potential for the occurrence of such a mechanism is currently under further investigation.

To determine the cellular location of the CR **1**-delivered Fl-AVWAL, COS-7 cells were grown on microscope slides. Unfixed cells were exposed to CR **1** (10 μM) and Fl-AVWAL (10 μM) in PBS for 1 h at 20 °C. Cells were examined by fluorescence microscopy (Zeiss Axioplan 2). Fl-AVWAL was seen in the cytoplasm and the nucleus of COS-7 cells (Figure 7). This result is consistent with our previous observation that the cytoplasm and nucleus of COS-7 cells are fluorescent when the cells are exposed to CR **1** and fluorescein.[13] Since small molecules (<9 nm in diameter), such as Fl-AVWAL, CR **1**, or the CR **1**·Fl-AVWAL complex, can pass into the nucleus through the nuclear pore complex by passive diffusion, it is not possible to determine whether CR **1** is involved in transport into the nucleus.[29] However, since the intensity of fluorescence in the nucleus does not directly correlate with that of the cytoplasm (Figure 7), nuclear delivery may be selectively aided by the presence of CR **1** in some cells by mechanisms that are not yet clear.

Conclusion

We have shown via NMR experiments that a cleft−[2]-rotaxane exists predominantly in an open conformation in apolar solutions and a closed conformation in aqueous solutions. These conformations arise from the wheel changing its position on the axle. Optimization of the rotaxanes' conformation is responsible for the favorable association of polar guests in buffered solutions and in DMSO and the transportation of guests through cell membranes. The results suggest that in the extracellular domain a noncovalent complex forms between CR **1** and Fl-AVWAL (Figure 8). The charged or polar functional groups that impede membrane penetration are covered or converted into a neutral form, and the complex passes through the lipid bilayer.

Locking the wheel in a closed conformation results in weaker interactions with fluorescein and Fl-AVWAL in an aqueous solution and in DMSO and inhibits CR **2**'s ability to deliver

(29) Gorlich, D.; Mattaj, I. W. *Science* **1996**, *271*, 1513−1518.

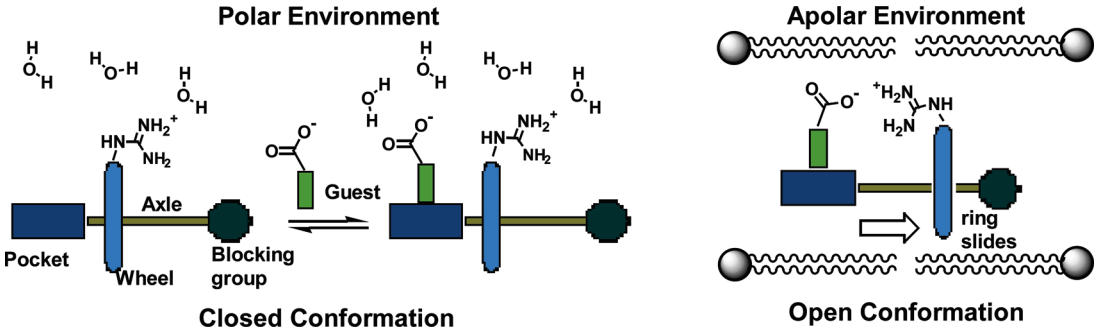

Figure 8. Host−rotaxanes alter their conformations, via the sliding motion of the wheel along the axle, in order to maximize the binding free energy of guest association and minimize the environmental effect on the stability of the complex, and in doing so enable the delivery of guests into cells.

Fl-AVWAL into cells. When a compound enters a cell, it experiences a decline in the polarity of the medium from bulk water ($\epsilon \approx 78$) to the alkyl chains of the phospholipids ($\epsilon \approx 2$) in the cell membrane.[17] The three solvent systems used in this study were chosen to mimic this environmental change. The poor binding in a DMSO-like environment, with a polarity similar to the cellular surface, most likely keeps CR **2** from being a transporter. CR **1**, however, alters its conformation, via the sliding motion of the wheel along the axle, in order to maximize the binding free energy of guest association and minimize the environmental effect on the stability of the complex, and in doing so enable the delivery of guests through the apolar cell membrane. This usage of rotaxanes as molecular machines that are amenable to the delivery of peptides directly into cells has the potential for significant clinical utility. Studies are currently underway to modify the properties of the rotaxanes in order to increase the favorable binding energy of rotaxane−guest complexes in cell-based systems, thereby improving intracellular transport efficiency.

Experimental Section

Determination of Association Constants Fluorescence quenching assays were performed to obtain the association constants. DMSO and $CHCl_3$ were freshly distilled and stored over molecular sieves (3 Å) prior to making the stock solutions and performing the assays. The water solution was buffered with phosphate (1 mM) at pH 7.0. 2.7 mL of these solutions were placed into a 3.5 mL cuvette. The guests were added to these solutions from a DMSO stock solution to give final concentrations of Fl-AVWAL (1.5×10^{-6} M), *N*-Ac-Trp (3.0×10^{-6} M), fluorescein (3.0×10^{-6} M), and pyrene (1.0×10^{-5} M). CR **1** or a CR **2** was dissolved in DMSO, and aliquots of these stock solutions were added to the cuvette in a 10^{-6} M increment from 1×10^{-6} M to 3×10^{-5} M. The total change in volume caused by addition of the guest and a rotaxane was less than 2%. The fluorescence spectrum was recorded and analyzed after each addition of a rotaxane. Plots of the changes observed in the quenching assays were fitted using a nonlinear least-squares procedure to derive K_A and ΔF_{max} values. The assays were duplicated, giving a standard deviation of less than 10% of the value obtained for the association constant.

Intracellular Transport Assays. COS-7 African green monkey kidney cells (ATCC CRL 1651) were propagated in Dulbecco's modified Eagle's medium (CellGro, MediaTech) and 10% fetal bovine serum (GIBCO/ InVitrogen). Cells were grown at 37 °C in a 5% CO_2 humidified incubator. Cells were subcultured 1:10 weekly.

Prior to assay, cells were grown in 6-well culture plates in DME with 10% fetal calf serum until they had reached 50−70% confluency (approximately 50 000 cells per well). After 24 h, the growth media was removed from the wells, and the cells were washed twice with phosphate-buffered saline (PBS, 11.9 mM phosphates, 137 mM NaCl, 2.7 mM KCl, pH 7.4). For the assays performed at room temperature, PBS buffer (1 mL) was added to each well. Aliquots of 5 mM stock solutions of CR **1** or CR **2** in DMSO were added to the wells to give the final concentrations as shown in Table 2 and 3. A baseline level of fluorescence was obtained from wells containing Fl-AVWAL only (10 or 20 μM). Other wells contained no reagents except DMSO (referred to as untreated cells). DMSO was added to the wells containing Fl-AVWAL and untreated cells to obtain an equivalent level of DMSO throughout the assays of 0.4%. The plates were rotated gently at rt for 30 min on a shaking platform. Fl-AVWAL was added (10 or 20 μM) to each well except for the one containing the untreated cells. The plates were rotated gently at room temperature in the dark for 1 h. Assay solutions were removed, and the cells were washed with 2 changes of 1 mL PBS and rotated gently for 2×10 min in the dark. The final washing solution was removed, and 1 mL of calcein blue AM solution (1 μM in PBS) was added to each well. After 10 min, cells were observed by inverted fluorescence microscopy (Zeiss Axiovert 200M). The cells were then harvested with trypsin versene (1 mL of a solution containing 0.25% trypsin, 0.01% EDTA incubated at 37 °C for 10 min) for flow cytometry. The cells were pelleted via centrifugation (5 min at 600 $\times G$). After removing the PBS solution, the cells were resuspended in FACS buffer (1% fetal bovine serum in PBS), and the proportion of fluorescent cells was measured using two-color flow cytometry (BD FACSAria).

To set thresholds, a control population of COS-7 cells was exposed to FAVWAL (10 μM) only. The threshold for background fluorescence was set at a position that included 5% of cells incubated with FAVWAL alone. The threshold for intensely positive fluorescence was set an arbitrary point at which one-third of the cells in the most highly fluorescent group (FAVWAL and CR **1**) were included. These thresholds were then applied to each sample tested. Dead cells and other debris were eliminated from analysis by preset gates.

Determination of fluoresceinated peptide localization in cells was achieved by high magnification microscopy. COS-7 cells were grown on 11×11 mm^2 glass coverslips (Corning) in a 6-well culture plate with one slide per well. Cells were exposed to CR **1** (10 μM) and Fl-AVWAL (10 μM) in the culture plate, as described above. The coverslips were then mounted onto microscope slides with Permafluor aqueous mounting medium (ThermoShandon). The unfixed cells were examined at 400× magnification by fluorescence microscopy (Zeiss Axioplan 2).

For cells assayed at 4 °C, the plates were stored at 4 °C for 15 min before the addition of CR **1**. The same procedure as that above was followed with the plates maintained at 4 °C except for the final wash step, which was performed at room temperature.

For depletion of cellular ATP, the cells were preincubated with 2-deoxy-D-glucose (6 mM) and sodium azide (10 mM) in PBS for 1 h, as described.[28] CR **1** was added to the solution containing 2-deoxy-D-glucose and sodium azide. After 30 min, Fl-AVWAL was added to this solution. After a 1 h incubation in PBS containing 2-deoxy-D-

glucose and sodium azide, the cells were washed and assayed using the same procedures as those described above.

Acknowledgment. This material is based upon work supported by the National Science Foundation under Grant No. CHE-0400539 and the American Cancer Society, Ohio Division, Inc. (A.F.D.). We thank Dr. David R. Plas for assistance in performing and analyzing the FACS experiments.

Supporting Information Available: General experimental procedures, synthetic procedure for CR **2**, one- and two-dimensional NMR spectra of CR **1** and CR **2**, molecular modeling of CR **1**, photographs of cells exposed to CR **1** and CR **2**. This material is available free of charge via the Internet at http://pubs.acs.org.

JA063667F